

Adsorption kinetics of herbicide paraquat from aqueous solution onto activated bleaching earth

W.T. Tsai ^{*}, C.W. Lai, K.J. Hsien

Department of Environmental Engineering and Science, Chia Nan University of Pharmacy and Science, Tainan 717, Taiwan

Received 26 June 2003; received in revised form 4 November 2003; accepted 11 November 2003

Abstract

In the present study, the activated bleaching earth was used as adsorbent for the herbicide paraquat adsorption in a batch adsorber. The rate of adsorption has been investigated under the controlled process parameters like agitation speed, initial paraquat concentration, adsorbent dosage and temperature. A batch kinetic model, based on the assumption of a pseudo-second order mechanism, has been tested to predict the rate constant of adsorption, equilibrium adsorption capacity, time of half-adsorption, and equilibrium concentration by the fittings of the experimental data. The results of the kinetic studies show that the adsorption process can be well described with the pseudo-second order equation. Based on the isotherm data obtained from the fittings of the adsorption kinetics, Freundlich model appears to fit the adsorption better than Langmuir model. In addition, the effective diffusion coefficient has also been estimated based on the restrictive diffusion model.

© 2003 Elsevier Ltd. All rights reserved.

Keywords: Activated bleaching earth; Paraquat; Liquid-phase adsorption; Kinetic modeling; Effective diffusion coefficient

1. Introduction

Paraquat (1,1'-dimethyl-4,4'-dipyridinium chloride), also known as methyl viologen, is frequently used as a quaternary ammonium herbicide due to its excellent action within plant cells (Khan, 1980). However, it is known that this compound is one of the most toxic poisons if deliberately or accidentally ingested (WHO, 1984; Chen and Lua, 2000). There have been many authenticated cases of the detection of its residues in water sources (Khan, 1980; Ritter et al., 2002). Regarding regulatory frameworks of pesticides in drinking water and effluent, it has been developed to protect the health of humans and the environment resulting from exposure to paraquat because it is the most widely used herbicide in Taiwan. For example, the

maximum contaminant level (MCL) has been set at 0.01 mg/l according to the drinking water standard.

There are two principal treatment processes for removal of paraquat in water and wastewater: destructive processes such as destructive oxidation (Andreozzi et al., 1993; Moctezuma et al., 1999; Lee et al., 2002; Kang, 2002), and recuperative processes such as adsorption into porous solids (Gonzalez-Pradas et al., 1997; Nakamura et al., 1999; Tsai et al., 2002). For virtually all pesticides, granular activated carbon (GAC) filter has been considered as the best available technology (AWWA, 1990). However, an important feature of cationic paraquat is to adsorb strongly on clay minerals, and somewhat less on activated carbon due to its highly polar nature of an expanding lattice clay, like montmorillonite (de Keizer, 1990). Retention by adsorption at a solid/liquid interface depends on the natures of both paraquat and clay and on the medium conditions (Draoui et al., 1999). Clays are the main components of the mineral fraction of soils. They are effective natural adsorbents due to their particle size (lower than 2 μm),

^{*} Corresponding author. Tel.: +886-6-2660393; fax: +886-6-2669090.

E-mail address: wtsai@mail.chna.edu.tw (W.T. Tsai).

Nomenclature

C_0	initial concentration of paraquat solution (mg/l)	q_e	amount of paraquat adsorbed at equilibrium (mg/g)
C_t	liquid-phase concentration of paraquat solution at t time (mg/l)	q_t	amount of paraquat adsorbed at time t (mg/g)
D_b	bulk diffusion coefficient (m^2/s)	$t_{1/2}$	time required for the adsorbent to take up half as much paraquat as it will at equilibrium (min)
D_e	effective diffusion coefficient (m^2/s)	V	volume of paraquat solution (l or dm^3)
$F(\lambda)$	function dependent on the ratio of critical molecular size and pore size (i.e., λ) (–)	W	mass of dry adsorbent used (g)
k	pseudo-second order rate constant (g/mg min)	ε	porosity of the porous particle (–)
		τ	tortuosity factor of the porous particle (–)

lamellar structures and negatively charged surfaces, which make them good adsorbents by ion exchange (Draoui et al., 1999). Thus, treatment of paraquat detoxification or the environmental fate of paraquat in the water/soil system is directed towards the contact with clay or earth (i.e., Fuller's earth or bentonite) (Khan, 1980; WHO, 1984).

In our previous studies (Tsai et al., 2002, 2003a,b), we investigated the adsorption isotherm of paraquat on activated bleaching earth (ABE) through batch-shaking method, and the kinetics of the adsorption system under the controlled process parameters like pH, salinity and particle size of ABE. Typical high-affinity isotherms (i.e., Type-H isotherms) were obtained at various conditions. Also, the adsorption kinetic of herbicide paraquat can be well described with the pseudo-second order model based on the strong electrostatic or ion-exchange interaction between the negatively charged surface and cationic paraquat (Khan, 1980). Obviously, it is necessary to further study the effects of the other system parameters on the adsorption kinetics as it provides significant insights into mechanisms of adsorption reaction in the wastewater treatment process and thus obtains appropriate residence time for the optimal removal of any pollutant from aqueous solutions. Thus, the present work aims to study the adsorption kinetics of herbicide paraquat on ABE used as adsorbent and to determine the factors controlling the adsorption rate. The effects of stirring speed, initial paraquat concentration, adsorbent dosage, and adsorption temperature on paraquat adsorption rate have been investigated. The pseudo-second order model is still adopted to evaluate its usefulness for describing the adsorption system. Further, the applicability of common isotherm models (i.e., Langmuir and Freundlich) also has been evaluated based on the adsorption capacities from the fittings of the pseudo-second order adsorption rate model. In addition, this paper also determines the effective diffusion coefficient in the ABE-paraquat adsorption system, which was estimated based on the restrictive diffusion model.

2. Materials and methods

2.1. Materials

The adsorbate used in the adsorption experiments is paraquat with purity of minimum 99%, which was purchased from Sigma Chemical Co. (St. Louis, USA). The molecular sizes of paraquat are about $1.34 \text{ nm} \times 0.36 \text{ nm}$ (Draoui et al., 1999). Activated bleaching earth (ABE) employed as adsorbent in the present study was obtained from an edible oil workshop (Taiwan Sugar Co., Kaohsiung, Taiwan). Its chemical composition of ABE measured by an inductively coupled plasma-atomic emission spectrometer (Model OPT 1MA 3000DA, Perkin Elmer Co., USA) is listed in Table 1. Analyses of pore properties of the clay adsorbent were measured at liquid nitrogen temperature (i.e., -196°C) using an ASAP 2010 apparatus (Micromeritics Co., USA). The reference sample (i.e., silica-alumina) from ASAP 2010 manufacturer was used to check the analysis quality by standard operational procedures before being measured in the experiments, which ensures continued accuracy of results. The true density (ρ_s) of the sample was measured by a helium displacement method with an AccuPyc 1330 pycnometer (Micromeritics Co., USA). From the data of total pore volume (V_t) and ρ_s , particle

Table 1
Chemical properties of activated bleaching earth (ABE) used as adsorbent in this study

Constituent (%)	Value (wt.%)
SiO ₂	72.9
Al ₂ O ₃	3.49
Fe ₂ O ₃	1.37
MgO	0.71
CaO	0.34
Na ₂ O	0.34
TiO ₂	0.22
K ₂ O	0.24

Table 2
Physical properties of ABE used as adsorbent in this study

Physical property	Value ^a
BET surface area (m ² /g), S_{BET}	263.0 ± 6.5
Micropore area (m ² /g), S_{mic}	14.1 ± 5.0
Total pore volume (cm ³ /g), V_t	0.369 ± 0.015
Micropore volume (cm ³ /g), V_{mic}	0.0053 ± 0.0001
Average pore diameter (Å) ^b , D_{ave}	56.1
True density (g/cm ³), ρ_s	2.3856 ± 0.0014
Particle density (g/cm ³) ^c , ρ_p	1.269
Particle porosity (–) ^d , ε_p	0.468

^a The data denote the mean ± standard deviation for at least two determinations.

^b The average pore diameter (D_{ave}) is approximately estimated by $4V_t/S_{\text{BET}}$ (Smith, 1981).

^c The particle density (ρ_p) is calculated from the total pore volume (V_t) and true density (ρ_s), i.e., $\rho_p = 1/[V_t + (1/\rho_s)]$.

^d The particle porosity (ε_p) is computed from the particle density (ρ_p) and true density (ρ_s), i.e., $\varepsilon_p = 1 - (\rho_p/\rho_s)$.

Table 3
Pore structures of ABE used as adsorbent in this study^a

Pore structure	Cumulative pore volume (cm ³ /g)	Cumulative pore surface (m ² /g)
Macropore (>500 Å)	0.056	4.0
Mesopore area (<500, > 20 Å)		
>400 Å	0.073	6.0
>300 Å	0.087	8.0
>200 Å	0.110	12.0
>100 Å	0.155	27.0
>80 Å	0.172	37.0
>60 Å	0.221	56.0
>40 Å	0.272	102.0
>20 Å	0.357	222.0
Micropore area (>17, <20 Å)	0.370	248.0

^a Based on Barrett–Joyner–Halenda (BJH) adsorption pore distribution data of one measurement.

density (ρ_p) and porosity (ε_p) can be further obtained (Smith, 1981). As given in Tables 2 and 3, obviously the clay adsorbent is a characteristic of mesoporous structure.

2.2. Methods

All of experiments of adsorption kinetics were carried out in a stirred batch adsorber shown in Fig. 1. The adsorber was immersed in a refrigerated circulating-water bath for isothermal condition prior to the experiment. For each experiment, 2.0 l of the paraquat solution were continuously stirred with a certain amount of the adsorbent dried in an oven (105 °C) for more than 24 h. A preliminary experiment revealed that 60–120

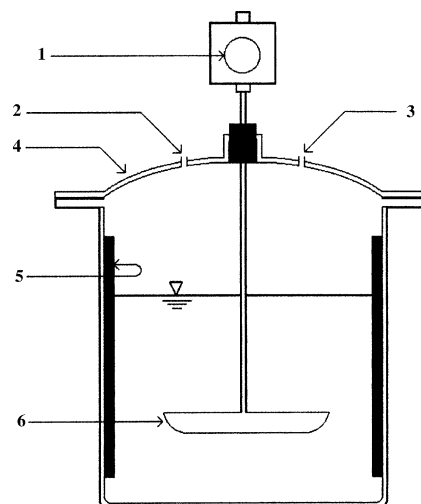


Fig. 1. Schematic diagram of the 3-l batch adsorber: 1. variable speed agitator; 2. sampling hole; 3. pH/temperature monitoring hole; 4. cover; 5. baffles; 6. Teflon impeller.

min time is required for the adsorption process to reach the equilibrium concentration. Thus, each sample of the solution (ca. 15 cm³) was withdrawn from the adsorber by a 20 ml syringe at intervals of 0.5, 1.0, 2.0, 5.0, 10.0, 30.0, 60.0, and/or 120.0 min. It was then filtrated with fiber membrane (Cat. No.: A045A025A; ADVANTEC MFS, Inc.). The concentration analysis of filtrate paraquat solution after adding sodium dithionite was immediately made with 1.0 cm light path quartz cells using spectrophotometer (Shimadzu UV-1201) at λ_{max} of 600 nm (AOAC, 1998). The amount of paraquat adsorbed was determined as follows:

$$q_t = (C_0 - C_t) \cdot V/W \quad (1)$$

where C_0 and C_t are the initial and liquid-phase concentrations of paraquat solution at t time (mg/l), respectively, V is the volume of paraquat solution (ca. 2 l), and W is the mass of dry adsorbent used (g). The experimental parameters, such as the stirring rate (200, 400, and 600 rpm), the initial paraquat concentration (70, 100, and 115 mg/l), adsorbent dosage (0.125, 0.250, 0.375, and 0.500 g/l) and temperature (25 and 45 °C), were investigated in the present study. In each experiment, the adsorption was carried out under the conditions where one parameter changed at a time while the other parameters held constant. In order to evaluate the statistical significance of data in the kinetic experiments, a preliminary experiment was repeated under identical conditions. It is evident from Fig. 2 that the experimental errors between the run No. 1 and run No. 2 are very limited, showing that the reproducibility of the measurements is within 5%.

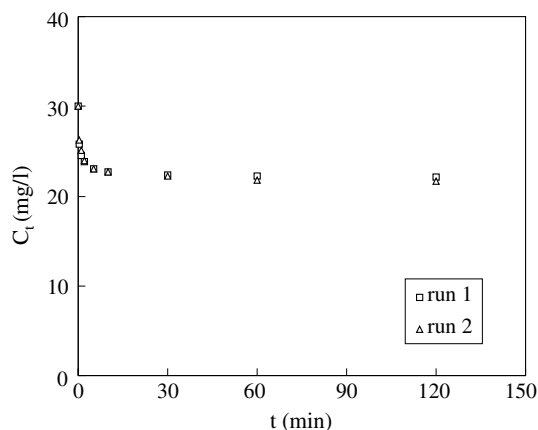


Fig. 2. Reproducibility test of variation of paraquat concentration vs. time (initial paraquat concentrations = 30 mg/l, adsorbent dosage = 0.5 g/l, agitation speed = 400 rpm, and temperature = 25 °C).

3. Results and discussion

3.1. Equilibrium time

The optimum period for the paraquat adsorption onto ABE can be observed by looking at the variances on paraquat concentration after adding the adsorbent. As shown in Fig. 3, preliminary investigations on the adsorption rate by the clay adsorbent have indicated that the process occurs rapidly. The decrease in residual paraquat concentration means the increase in amount of paraquat adsorbed as a function of time until the adsorption of paraquat approached to remain constant, implying adsorption equilibrium has been reached. After the lapse of 60–120 min, a gradual approach to the

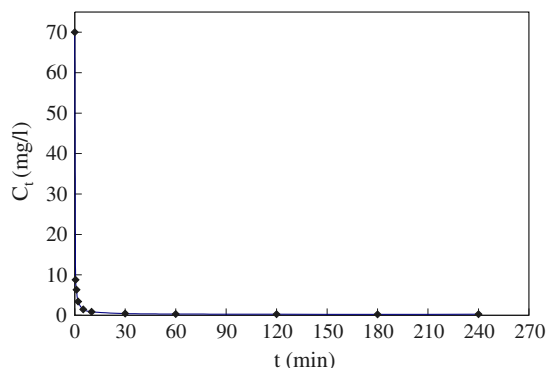


Fig. 3. Plot of concentrations of paraquat solution vs. time (initial paraquat concentrations = 70 mg/l, adsorbent dosage = 2 g/l, agitation speed = 400 rpm, and temperature = 25 °C).

limiting adsorption was observed. Therefore, the optimum agitation period for the removal of paraquat is about 60–120 min in the adsorption system. These results are still expected to show that ABE has a high affinity for this cationic herbicide in this study, which are consistent with their isotherms and the profiles of paraquat concentration in our previous studies (Tsai et al., 2002, 2003a,b).

3.2. Adsorption kinetics

The adsorption process of a porous adsorbent in a stirring chamber generally involves several transport stages (Noll et al., 1992; Al Duri, 1996); i.e., external diffusion, internal diffusion and actual adsorption process. The model of the separation process should adequately account for the mass balance and the equilibrium isotherm if the system is isothermal. In most cases, the resistance to internal diffusion can be significant. However, the local rate of adsorption is assumed to be relatively fast and the resistance to external diffusion is experimentally controlled to be negligible, compared to the intra-particle diffusion. Although many theoretical model equations have been proposed for describing the adsorption kinetics based on mass balance, pore diffusion rate and initial/boundary conditions. These equations are not only complicated and impractical in industry, but also require detailed data such as the characteristics of adsorbate and adsorbent.

Due to the fast decrease in residual paraquat concentration at a short time scale, implying the strong electrostatic interaction between the negatively charged surface and paraquat cation, a simple kinetic analysis of adsorption, pseudo-second order equation, was thus used to fit experimental data in the present work (Ho and McKay, 2000; Ho and Chiang, 2001; Ho et al., 2001; Wu et al., 2001):

$$dq_t/dt = k(q_e - q_t)^2 \quad (2)$$

where k is the pseudo-second order rate constant (g/mg min), q_e is the amount of paraquat adsorbed at equilibrium (mg/g), q_t is the amount of paraquat adsorbed at time t (mg/g). Integrating Eq. (2) for the boundary conditions $t = 0$ to $t = t$ and $q_t = 0$ to $q_t = q_t$, gives:

$$1/(q_e - q_t) = 1/q_e + kt \quad (3)$$

Eq. (3) can be rearranged to obtain a linear form:

$$t/q_t = 1/(k \cdot q_e^2) + (1/q_e) \cdot t \quad (4)$$

Rate parameters, k and q_e , can be directly obtained from the intercept and slope of the plot of (t/q_t) against t . The equilibrium concentration (i.e., C_e) can be further calculated from Eq. (1) as the value of q_e has been obtained

from the fitting of Eq. (4). Also, half of the paraquat-adsorption time, $t_{1/2}$, is the time required for the adsorbent to take up half as much paraquat as it will at equilibrium (i.e., $t = t_{1/2}$ as $q_t = q_e/2$). This period of time is often used as a measure of the rate of adsorption and is given from the rearrangement of Eq. (3) as follows:

$$t_{1/2} = 1/(k \cdot q_e) \quad (5)$$

The effects of the stirring (mixing) speed, initial paraquat concentration, adsorbent mass, and temperature on the rate and extent of adsorption of ABE were studied and presented as below.

3.2.1. Effect of agitation speed

The effect of agitation speed on paraquat adsorption at the adsorbent dosage of 2 g/l and initial paraquat concentration of 30 mg/l is shown in Fig. 4 and Table 4. The correlation between the experiments with the theoretical results is excellent. The data listed in Table 4 indicates that the adsorption capacity (i.e., q_e) slightly increased and equilibrium concentration thus decreased as the agitation speed increased from 200 to 600 rpm. This effect can be attributed to the increase in turbulence and the decrease in boundary layer thickness around the adsorbent particles as a result of increase in the degree of

mixing (Weber and DiGiano, 1996). This result is also in agreement with those of Ho et al. (2001) and Al-Qodah (2000) for the dye of adsorption onto activated clay and shale oil ash, respectively.

3.2.2. Effect of initial concentration

The effect of the initial paraquat concentration on the intake rate by ABE adsorption at adsorbent dosage of 2 g/l and mixing speed of 400 rpm is shown in Fig. 5 where the experimental data are shown as discrete points and those obtained from the model by solid lines. It is evident from Fig. 5 that the rate of adsorption decreased with time until it gradually approached a plateau due to the continuous decrease in the concentration driving force. The kinetic data obtained from batch studies have been analyzed by using the pseudo-second order model. Values of k , q_e , correlation coefficient (R^2), $t_{1/2}$, and C_e for the paraquat adsorption system, computed from Eqs. (4), (5) and (1), are listed in Table 5, from which it will be seen that the kinetics of paraquat adsorption onto ABE follows this model with the regression coefficients of higher than 0.999 for all the system in this study. Clearly, the adsorption capacity (i.e., q_e) increased as the initial paraquat concentration (i.e., C_0) and equilibrium concentration (i.e., C_e) increased, which is also consistent with their adsorption isotherms in our

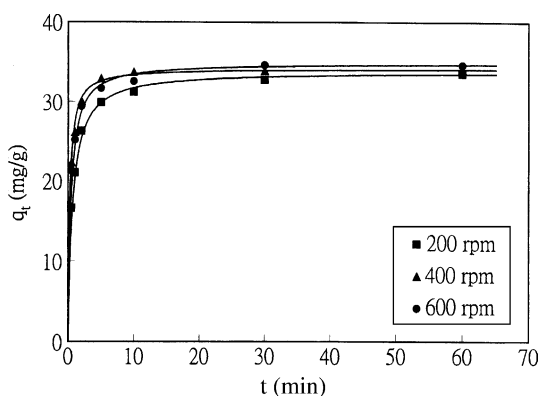


Fig. 4. Plots of adsorbed amount vs. time for various agitation speeds (initial paraquat concentrations = 30 mg/l, adsorbent dosage = 2 g/l, and temperature = 25 °C; symbols: experimental data, full lines: calculated from Eq. (3) and Table 4).

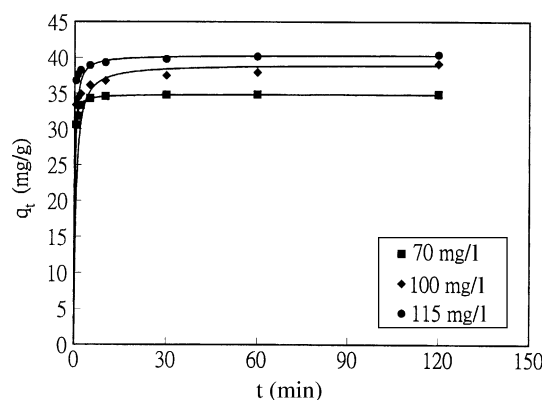


Fig. 5. Plots of adsorbed amount vs. time for various initial paraquat concentrations (adsorbent dosage = 2 g/l, agitation speed = 400 rpm, and temperature = 25 °C; symbols: experimental data, full lines: calculated from Eq. (3) and Table 2).

Table 4

Kinetic parameters for paraquat adsorption onto ABE at various agitation speeds^a

Agitation speed (rpm)	K (g/mg min)	q_e (mg/g)	Correlation coefficient	$t_{1/2}$ (min)	C_e (mg/l)
200	0.0437	33.898	0.9999	0.675	21.525
400	0.1184	34.247	1.0000	0.247	21.438
600	0.0660	34.965	1.0000	0.433	21.259

^a Adsorption conditions: initial concentration = 30 mg/l, adsorbent dosage = 2 g/l, and temperature = 25 °C.

Table 5

Kinetic parameters for paraquat adsorption onto ABE at various initial concentrations^a

C_0 (mg/l)	K (g/mg min)	q_e (mg/g)	Correlation coefficient	$t_{1/2}$ (min)	C_e (mg/l)
70	0.3295	34.843	1.0000	0.087	0.314
100	0.0482	39.063	0.9997	0.531	21.875
115	0.1230	40.323	1.0000	0.202	34.355

^a Adsorption conditions: adsorbent dosage = 2 g/l, agitation speed = 400 rpm, and temperature = 25 °C.

previous study (Tsai et al., 2002) and other studies (de Keizer, 1990; Gonzalez-Pradas et al., 1997; Draoui et al., 1999). Similar results were observed by Ho et al. (2001) for the adsorption system of dyes onto activated clay.

3.2.3. Effect of adsorbent mass

The effect of varying the ABE mass on paraquat adsorption at the initial paraquat concentration of 30 mg/l and mixing speed of 400 rpm is shown in Fig. 6. The values of parameters for the adsorption system have been obtained and listed in Table 6. It is evident from Fig. 6 that the correlation between the experimental and theoretical results is also good. It can be expected that the paraquat concentration in the solution decreased and the adsorbed amount thus increased at a faster rate as the adsorbent mass and/or adsorbent concentration

increased. Table 6 shows that the adsorption capacity (i.e., q_e) increased and equilibrium concentration thus decreased as the adsorbent mass and/or adsorbent concentration increased. This result is in agreement with those of El-Guendi (1991) and Al-Qodah (2000) for the adsorption of dye onto natural clay and shale oil ash, respectively.

3.2.4. Effect of adsorption temperature

The plots of q_t vs. t at 25 and 45 °C are shown in Fig. 7. The sorption process still confirms to fit the pseudo-second order model with high correlation coefficient (>0.99). Values of model parameters (i.e., k and q_e), $t_{1/2}$, and C_e for two temperatures are given in Table 7. It is clear that fitted sorption capacity at equilibrium (i.e., q_e) decreased with increasing temperature, that is, values

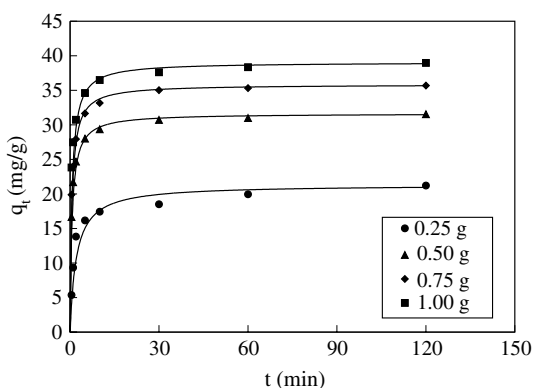


Fig. 6. Plots of adsorbed amount vs. time for various adsorbent dosages (initial paraquat concentrations = 30 mg/l, agitation speed = 400 rpm, and temperature = 25 °C; symbols: experimental data, full lines: calculated from Eq. (3) and Table 3).

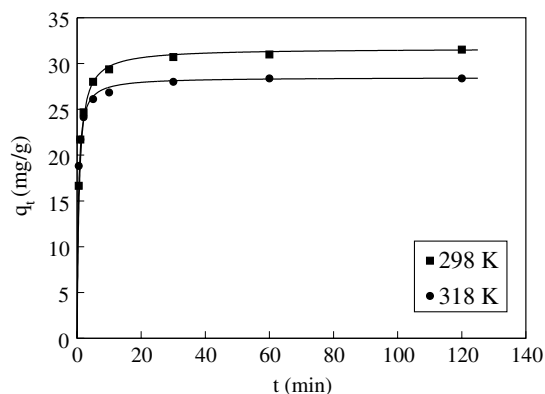


Fig. 7. Plots of adsorbed amount vs. time for 25 and 45 °C (initial paraquat concentrations = 30 mg/l, adsorbent dosage = 2 g/l and agitation speed = 400 rpm; symbols: experimental data, full lines: calculated from equation (3) and Table 3).

Table 6

Kinetic parameters for paraquat adsorption onto ABE at various adsorbent dosages^a

W/V (g/l)	K (g/mg min)	q_e (mg/g)	Correlation coefficient	$t_{1/2}$ (min)	C_e (mg/l)
0.125	0.0223	21.322	0.9988	2.103	24.670
0.250	0.0478	31.646	1.0000	0.661	22.089
0.375	0.0453	35.842	1.0000	0.616	21.039
0.500	0.0395	39.063	0.9999	0.648	20.234

^a Adsorption conditions: initial concentration = 30 mg/l, agitation speed = 400 rpm, and temperature = 25 °C.

Table 7
Kinetic parameters for paraquat adsorption on ABE at 25 and 45 °C^a

Temperature (°C)	<i>K</i> (g/mg min)	<i>q_e</i> (mg/g)	Correlation coefficient	<i>t</i> _{1/2} (min)	<i>C_e</i> (mg/l)
25	0.0478	31.646	1.0000	0.661	22.089
45	0.0893	28.490	1.0000	0.393	22.878

^a Adsorption conditions: initial concentration = 30 mg/l, adsorbent dosage = 0.25 g/l, and agitation speed = 400 rpm.

of *q_e* decreased from 31.65 mg/g at 25 °C to 28.49 mg/g at 45 °C. Furthermore, values of *C_e* increased with increasing temperature. Values of rate constant (i.e., *k*) and *t*_{1/2}, on the other hand, have an increase trend with increasing temperature. This observation is significantly consistent with that studied by Nakamura et al. (1999) where sorption capacity of paraquat was also found to decrease with increasing temperature in the case of activated carbon. Based on the above results, it implies that physical adsorption mechanism may play an important role in the paraquat–clay system. Further, increasing temperature usually increases the rate of approach to equilibrium but decreases the equilibrium capacity in the case of physical adsorption.

As a preliminary engineering application for the removal of paraquat from aqueous solution, activated bleaching earth is used in powdered form to adsorb the organic compound by using a continuous operation system, in that a rapid-mix basin with propeller–impeller device is designed to disperse the adsorbent uniformly throughout the basin and to allow adequate contact between the adsorbent particle and the paraquat adsorbate (Reynolds and Richards, 1996). Further, an example using these experimental results is as follows: if the influent containing paraquat to a propeller–impeller tank has a flow rate of 240 m³/day and concentration of 70 mg/l, the allowable effluent concentration = 1 mg/l (see Table 5), the agitating speed = 400 rpm, the system temperature = 25 °C, the adsorbent dosage = 2 g/l (= 2 kg/m³), and the residence time = 60 min (= 1/24 day), then the effective tank volume = 240 m³/day × 1/24 day = 10 m³ and adsorbent feeding rate = 240 m³/day × 2 kg/m³ = 480 kg/day = 20 kg/h.

3.3. Adsorption isotherms

It is practically important to establish the most appropriate correlations for the equilibrium data in the design of adsorption system. Two common isotherm

equations have been tested in the present study: Langmuir and Freundlich models.

$$\text{Langmuir: } 1/q_e = 1/[(K_L q_m)C_e] + 1/q_m \quad (6)$$

$$\text{Freundlich: } q_e = K_F \cdot C_e^{1/n} \quad (7)$$

In Eq. (6), *C_e* and *q_e* are as defined in Eq. (2), *K_L* is a direct measure for the intensity of the adsorption process (l/mg), and *q_m* is a constant related to the area occupied by a monolayer of adsorbate, reflecting the adsorption capacity (mg/g). From a plot of 1/*q_e* vs. 1/*C_e*, *q_m* and *K_L* can be determined from its slope and intercept. In Eq. (7), *K_F* is a constant for the system, related to the bonding energy. *K_F* can be defined as adsorption or distribution coefficient and represents the quantity of dye adsorbed onto adsorbents for a unit equilibrium concentration (i.e., *C_e* = 1 mg/l). The slope 1/*n*, ranging between 0 and 1, is a measure for the adsorption intensity or surface heterogeneity (Haghsresht and Lu, 1998; Fytianos et al., 2000). A plot of ln *q_e* vs. *C_e* enables the empirical constants *K_F* and 1/*n* to be determined from the intercept and slope of the linear regression. Judging the correlation coefficients, *R*², compares applicability of the isotherm equations.

Table 8 presents the results of Langmuir and Freundlich isotherm fits by using the adsorption capacity data from Table 5 at 25 °C. Obviously, it can be seen in Fig. 8 that the Freundlich model yields a somewhat better fit than the Langmuir model, as reflected with correlation coefficients (*R*²) of 0.9854 and 0.9640, respectively, which is consistent with our previous study (Tsai et al., 2002). As also illustrated in Table 8, the value of 1/*n* is 0.0294 that indicate a highly favorable adsorption isotherm.

3.4. Diffusion coefficient

According to the typical adsorption model (Noll et al., 1992; Al Duri, 1996), there are two main mass

Table 8
Isotherm parameters for adsorption of paraquat onto ABE in water solutions at 25 °C^a

Langmuir			Freundlich		
<i>q_m</i> (mg/g)	<i>K_L</i> (l/mg)	<i>R</i> ²	<i>K_F</i> [mg/g (l/mg) ^{1/n}]	1/ <i>n</i> (–)	<i>R</i> ²
39.68	22.91	0.9640	36.02	0.0294	0.9854

^a Isotherm data based on the fitting results of Table 5.

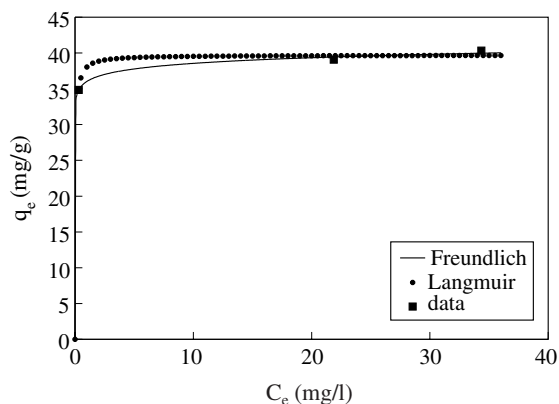


Fig. 8. Adsorption isotherms of paraquat onto ABE at 25 °C (symbols: data from the fittings of pseudo-second order adsorption kinetics or Table 5; full lines: calculated from Langmuir and Freundlich models).

transfer resistances, i.e., external diffusion across the boundary layer surrounding each adsorbent particle and internal diffusion into the porous particle. In the previous discussion, it seems that the effect of agitation speed on the rate and capacity of adsorption is negligible in this investigation, implying that the rate of adsorption in the porous adsorbent should be controlled by transport within the pore network. For the liquid-phase diffusion of an adsorbate with large molecular size in porous materials, its effective diffusion coefficient (D_e) can be related to the equation describing the restrictive or hindered diffusion (Chantong and Massoth, 1983; Smith, 1986) as follows:

$$D_e = [D_b \cdot \varepsilon / \tau] \cdot F(\lambda) \quad (8)$$

where D_b is the bulk diffusion coefficient in free solution using Hayduk and Laudie method for estimation (Lyman et al., 1982), ε is the porosity, τ is the tortuosity factor of the porous particle ranging from 2 to 6 (Smith, 1981), and $F(\lambda)$ is a function dependent on the ratio of critical molecular size and pore size (i.e., λ) accounting for steric hindrance/exclusion and hydrodynamic drag effects. In the present study, the value of λ is approximately equal to 0.0673 ($=0.36 \text{ nm}/5.61 \text{ nm}$) (Draoui et al., 1999). For small λ (<0.1), Brenner and Gaydos (1977) have shown

$$F(\lambda) = 1 + (9/8) \cdot \lambda \cdot \ln(\lambda) - 1.54\lambda \quad (9)$$

D_e for the intra-particle transport of paraquat within the pores of ABE has been estimated to $1.029 \times 10^{-6} \text{ cm}^2/\text{s}$ based on $D_b = 6.692 \times 10^{-6} \text{ cm}^2/\text{s}$, $\varepsilon = 0.468$, τ ($\approx 1/\varepsilon$) = 2.14 (Smith, 1981) and $F(\lambda) = 0.703$. The obtained value of the effective diffusivity is compared to those found in literatures (Al Duri, 1996; Al-Qodah, 2000).

4. Conclusions

The use of activated bleaching earth for the adsorption of paraquat from aqueous solution has been examined. The following conclusions can be drawn:

- Initially, the rate of adsorption of paraquat onto the clay adsorbent is very fast. This is then followed by a slower rate, and gradually approaches a plateau.
- The adsorption kinetics can be well described by the pseudo-second order model equation.
- The effect of the initial paraquat concentration, adsorbent dosage and adsorption temperature on the rate of adsorption and the equilibrium adsorption was found to be of considerable significance.
- The intra-particle diffusion mechanism plays a significant role in the adsorption system based on the results of the effect of agitation speed on the rate of adsorption and the equilibrium adsorption capacity.
- The results of this research were found to be in agreement with those of the similar adsorption system.
- The effective diffusion coefficient, estimated based on the restrictive diffusion model, is compared to the published data in literature.

Acknowledgements

This research was supported by NSC (National Science Council), Taiwan, under contract number NSC 90-2211-E-041-010.

References

- Al Duri, B., 1996. Adsorption modeling and mass transfer. In: McKay, G. (Ed.), Use of Adsorbents for the Removal of Pollutants from Wastewaters. CRC Press, Boca Raton, FL, USA.
- Al-Qodah, Z., 2000. Adsorption of dyes using shale oil ash. Water Res. 34, 4295–4303.
- American Water Works Association (AWWA), 1990. Water Quality and Treatment, fourth ed., McGraw-Hill, New York, NY, USA.
- Andreozzi, R., Insola, A., Caprio, V., D'Amore, M.G., 1993. Ozonation of 1,1'-dimethyl-4,4'-bipyridinium dichloride (paraquat) in aqueous solution. Environ. Technol. 14, 695–700.
- AOAC Official Method 969.09, 1998. Paraquat in pesticide formulations (spectrophotometric method), Official Methods of Analysis of AOAC International, 16th ed., AOAC International, Arlington, VA, USA.
- Brenner, H., Gaydos, L.J., 1977. The constrained brownian movement of spherical particles in cylindrical pores of comparable radius. J. Colloid Interface Sci. 58, 312–356.
- Chantong, A., Massoth, F.E., 1983. Restrictive diffusion in aluminas. AIChE J. 29, 725–731.
- Chen, C.M., Lua, A.C., 2000. Lung toxicity of paraquat in the rat. J. Toxicol. Environ. Health (A) 59, 477–478.

- de Keizer, A., 1990. Adsorption of paraquat ions on clay minerals: electrophoresis of clay particles. *Progr. Colloid Polym. Sci.* 83, 118–126.
- Draoui, K., Denoyel, R., Chgoura, M., Rouquerol, J., 1999. Adsorption of paraquat on minerals: a thermodynamic study. *J. Therm. Anal. Cal.* 58, 597–606.
- El-Guendi, M., 1991. Homogeneous surface diffusion model of basic dyestuffs onto natural clay in batch adsorbers. *Adsorption Sci. Technol.* 8, 217–225.
- Fytianos, K., Voudrias, E., Kokkalis, E., 2000. Sorption–desorption behavior of 2,4-dichlorophenol by marine sediments. *Chemosphere* 40, 3–6.
- Gonzalez-Pradas, E., Villafranca-Sanchez, M., Gallego-Campo, A., Urena-Amate, D., Socias-Viciano, M., 1997. Removal of 1,1'-dimethyl-4,4'-bipyridinium dichloride from aqueous solution by natural and activated bentonite. *J. Chem. Tech. Biotechnol.* 69, 173–178.
- Haghsereht, F., Lu, G., 1998. Adsorption characteristics of phenolic compounds onto coal-reject-derived adsorbents. *Energy Fuels* 12, 1100–1107.
- Ho, Y.S., Chiang, C.C., 2001. Sorption studies of acid dye by mixed sorbents. *Adsorption* 7, 139–147.
- Ho, Y.S., McKay, G., 2000. The kinetics of sorption of divalent metal ions onto sphagnum moss peat. *Water Res.* 34, 735–742.
- Ho, Y.S., Chiang, C.C., Hsu, Y.C., 2001. Sorption kinetics for dye removal from aqueous solution using activated clay. *Sep. Sci. Technol.* 36, 2473–2488.
- Kang, M., 2002. Preparation of TiO₂ photocatalyst film and its catalytic performance for 1,1'-dimethyl-4,4'-bipyridinium dichloride decomposition. *Appl. Catal. (B)* 37, 187–196.
- Khan, S.K., 1980. *Pesticides in the Soil Environment*. Elsevier, Amsterdam.
- Lee, J.C., Kim, M.S., Kim, B.W., 2002. Removal of paraquat dissolved in a photoreactor with TiO₂ immobilized on the glass-tubes of UV lamps. *Water Res.* 36, 1776–1782.
- Lyman, W.J., Reehl, W.F., Rosenblatt, D.H., 1982. *Handbook of Chemical Property Estimation Methods*. American Chemical Society, Washington, DC.
- Moctezuma, E., Leyva, E., Monreal, E., Villegas, N., Infante, D., 1999. Photocatalytic degradation of the herbicide paraquat. *Chemosphere* 39, 511–517.
- Nakamura, T., Kawasaki, N., Ogawa, H., Tanada, S., Kogirima, M., Imaki, M., 1999. Adsorption removal of paraquat and diquat onto activated carbon at different adsorption temperature. *Toxicol. Environ. Chem.* 70, 275–280.
- Noll, K.E., Gounaris, V., Hou, W.S., 1992. *Adsorption Technology for Air and Water Pollution Control*. Lewis, Chelsea, USA.
- Reynolds, T.D., Richards, P.A., 1996. *Unit Operations and Processes in Environmental Engineering*, second ed. PWS Publisher, Boston, MA, USA.
- Ritter, L., Solomon, K., Sibley, P., Hall, K., Keen, P., Mattu, G., Linton, B., 2002. Sources, pathways, and relative risks of contaminants in surface water and groundwater: a perspective prepared for the Walkerton inquiry. *J. Toxicol. Environ. Health (A)* 65, 1–142.
- Smith, J.M., 1981. *Chemical Engineering Kinetics*, third ed. McGraw-Hill, New York, USA.
- Smith, D.M., 1986. Restricted diffusion through pores with periodic constrictions. *AIChE J.* 32, 1039–1042.
- Tsai, W.T., Hsieh, M.F., Sun, H.F., Chien, S.F., Chen, H.P., 2002. Adsorption of paraquat onto activated bleaching earth. *Bull. Environ. Contam. Toxicol.* 69, 189–194.
- Tsai, W.T., Lai, C.W., Hsien, K.J., 2003a. Effect of particle size of activated clay on the adsorption of paraquat from aqueous solution. *J. Colloid Interface Sci.* 263, 29–34.
- Tsai, W.T., Lai, C.W., Hsien, K.J., 2003b. The effects of pH and salinity on kinetics of paraquat sorption onto activated clay. *Colloid Surf. (A)* 224, 99–105.
- Weber Jr., W.R., DiGianno, F.A., 1996. *Process Dynamic in Environmental Systems*. John Wiley & Sons, New York, NY, USA.
- WHO, 1984. *Paraquat and Diquat*, World Health Organization, Geneva, Switzerland, pp. 42–128.
- Wu, F.C., Tseng, R.L., Juang, R.S., 2001. Kinetic modeling of liquid-phase adsorption of reactive dyes and metal ions on chitosan. *Water Res.* 35, 613–618.